

## Supporting Information for

# Ultra-sensitive detection of human chorionic gonadotropin using frequency locked microtoroid optical resonators

*Erol Ozgur<sup>1</sup>, Kara Ellen Roberts<sup>1</sup>, Ekin Ozge Ozgur<sup>1</sup>, Adley Nathanael Gin<sup>2</sup>, Jaden Robert Bankhead<sup>2</sup>, Zhikun Wang<sup>2</sup>, and Judith Su<sup>1,2\*</sup>*

<sup>1</sup>Department of Biomedical Engineering, The University of Arizona, Tucson, AZ 85721

<sup>2</sup>Wyant College of Optical Sciences, The University of Arizona, Tucson, AZ 85721

### **Corresponding Author**

Corresponding Author's Email: [judy@optics.arizona.edu](mailto:judy@optics.arizona.edu), Phone: (+1) 520-621 4240

### **Table of Contents**

Fig. S1. Measurement of hCG levels in urine samples using commercial pregnancy strips.	pg. S-2
Error analysis for Fig 3b.	pg. S-2
Fig. S2. Filtering of optical data.	pg. S-3
Fig. S3. Relationship between temperature and resonance wavelength shift.	pg. S-4
Fig. S4. Simultaneous wavelength and temperature measurement.	pg. S-5

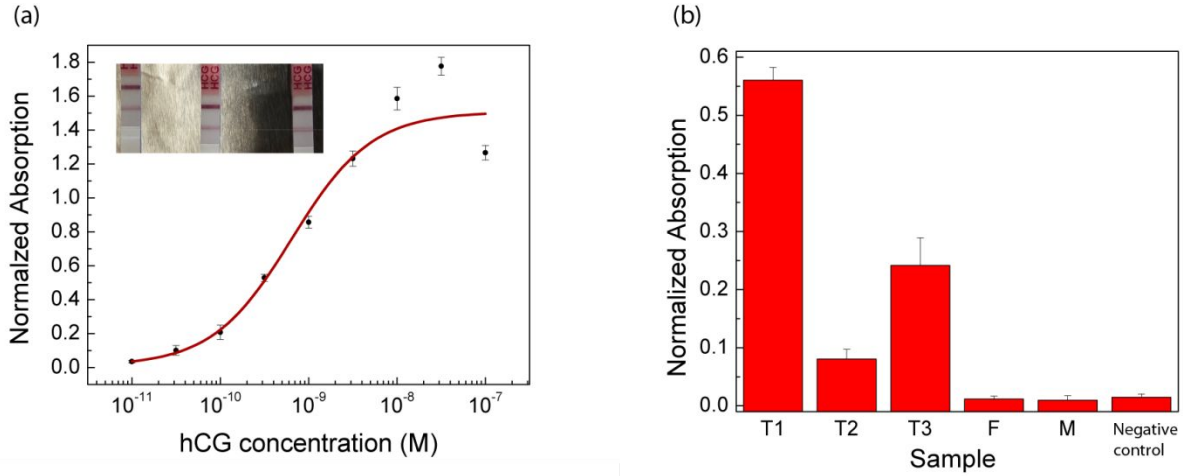


**Figure S1. Measurement of hCG levels in urine samples using commercial pregnancy strips.** (a) To determine the hCG concentration in the urine samples a calibration curve was prepared using commercial pregnancy test strips. hCG was diluted to various concentrations in simulated urine. The strips were dipped into these solutions with known hCG concentration. Images of the test strips (inset) were taken under the same illumination conditions using a smartphone camera. The absorption values were plotted for the average and standard deviation of 3 test strips, and the calibration curve was formed by sigmoidal fitting. The highest three concentrations show deviation from the sigmoidal pattern, yet; concentrations below 10 nM show good correlation with the expected value, and we only apply this calibration curve for samples with concentration below 10 nM. (b) The absorption levels measured from urine samples obtained from single donors, which are at first (T1), second (T2), and third (T3) trimesters of pregnancy, as well as non-pregnant female (F) and male (M) donors. The negative control is the simulated urine. To prevent the concentrations from exceeding the reliable measurement range of pregnancy test strips, samples were diluted 100 times in simulated urine before the measurement. The values correspond to hCG concentrations of 37 nM, 3 nM, and 11 nM in the three semesters of pregnancy.

### Error analysis for Fig. 3d.

The equation for the logistic curve fit for absorbance ( $A$ ) shown in Fig S2(a) is given by

$$A = f(x) = B_2 + \frac{B_1 - B_2}{1 + \left(\frac{x}{x_0}\right)^p}$$

Then, we can define:

$$g(A; x_0, B_1, B_2, p) = f^{-1}(A)$$

Standard error propagation results in:

$$\sigma_x^2 = \sigma_A^2 \left(\frac{\partial g}{\partial A}\right)^2 + \sigma_{x_0}^2 \left(\frac{\partial g}{\partial x_0}\right)^2 + \sigma_{B_1}^2 \left(\frac{\partial g}{\partial B_1}\right)^2 + \sigma_{B_2}^2 \left(\frac{\partial g}{\partial B_2}\right)^2 + \sigma_p^2 \left(\frac{\partial g}{\partial p}\right)^2$$

The error bars in Fig. 3d are  $\pm\sigma_x$ . The values for  $\sigma_{x_0}, \sigma_{B_1}, \sigma_{B_2}, \sigma_p$  are obtained from the 68% confidence interval bounds from the fit in Fig S2(a) and are  $3.27 \times 10^{-10}$ , 0.160, 0.140, and 0.484 respectively. The fit parameters are  $x_0 = 7.26 \times 10^{-10}$ ;  $B_1=0.045$ ;  $B_2=1.56$ ; and  $p=1.07$ . The mean absorbance values are: 0.560, 0.081, and 0.242 for trimesters 1, 2, and 3 respectively.

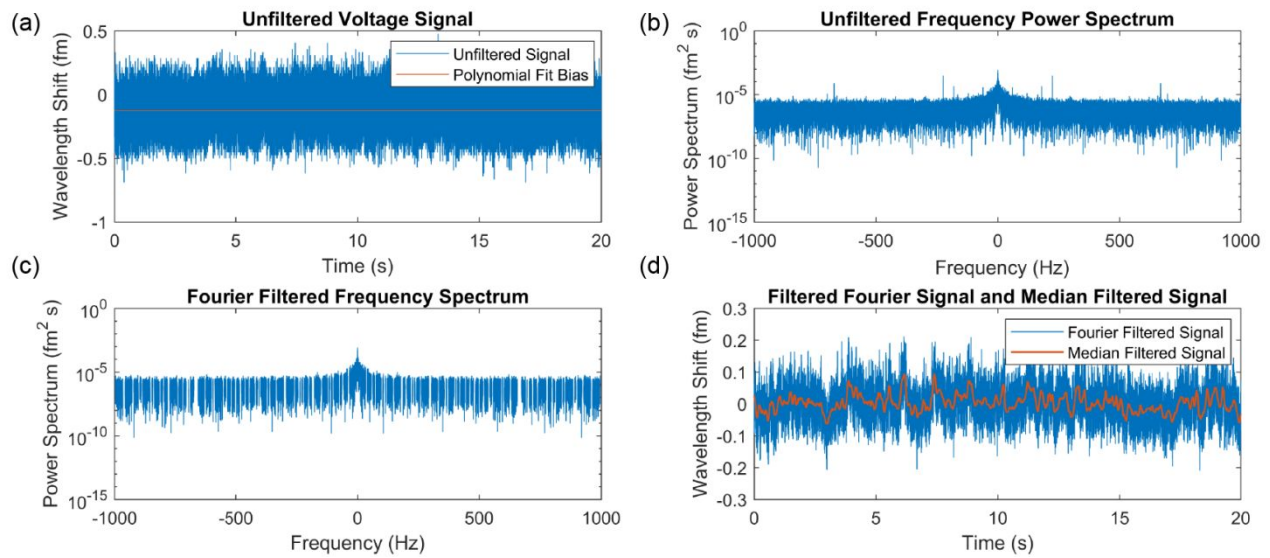


**Figure S2. Filtering of the optical data.** (a), The measurement performed in this graph is a background noise measurement of the inherent stability of the laser. (b), The data is Fourier transformed. Peaks in the spectrum correspond to periodic noise. These frequencies, including 60 Hz electrical line noise, and their multiples are filtered using a custom-built script. All the data above 1 kHz is also filtered because of the dither signal at 2 kHz, and because we are not interested in events occurring at time scales on the order of 1 ms or shorter. (c), The Fourier spectrum after filtering. (d) Inverse Fourier transformed data after filtering, drawn in blue. After Fourier filtering, a median filter is applied to the data.

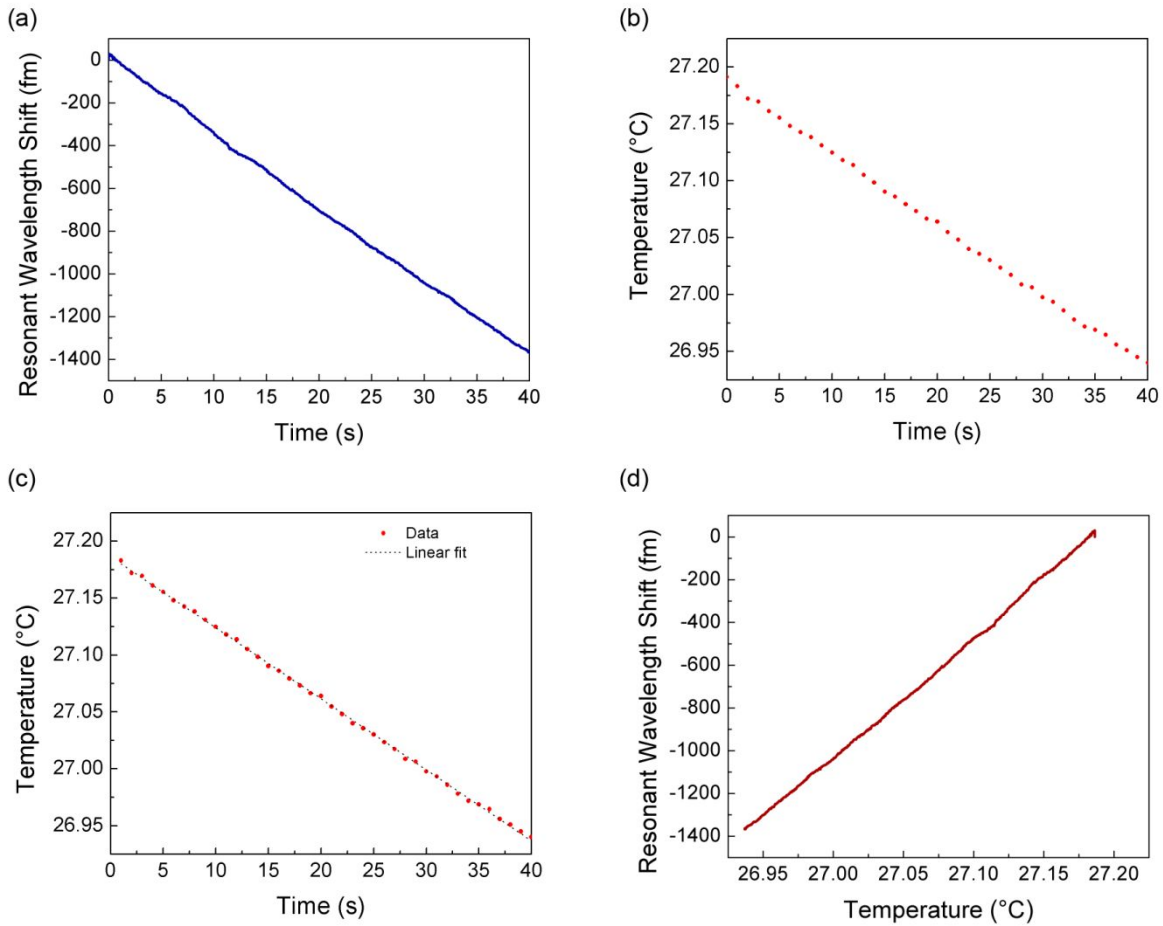


**Figure S3. Relationship between temperature and resonance wavelength shift.** To determine the effect of temperature on resonance wavelength shift, a microtoroid was immersed in water and heated to 28°C using a PID-controlled heater embedded into the measurement stage. The heater was then turned off, and as the system cooled, the resonance frequency of the toroid was tracked. (a) The wavelength shift with respect to time is linear over a range of at least 40 s. (b) The temperature of the sample chamber as measured by a thermocouple positioned near the toroid. (c) A linear fit of the temperature measurement. The  $r^2$  value of the linear fit is 0.9995. (d) The wavelength fit plotted as a function of temperature. It has a linear relationship with respect to temperature. A temperature change of 1°C corresponds to a wavelength shift of approximately 5 pm.

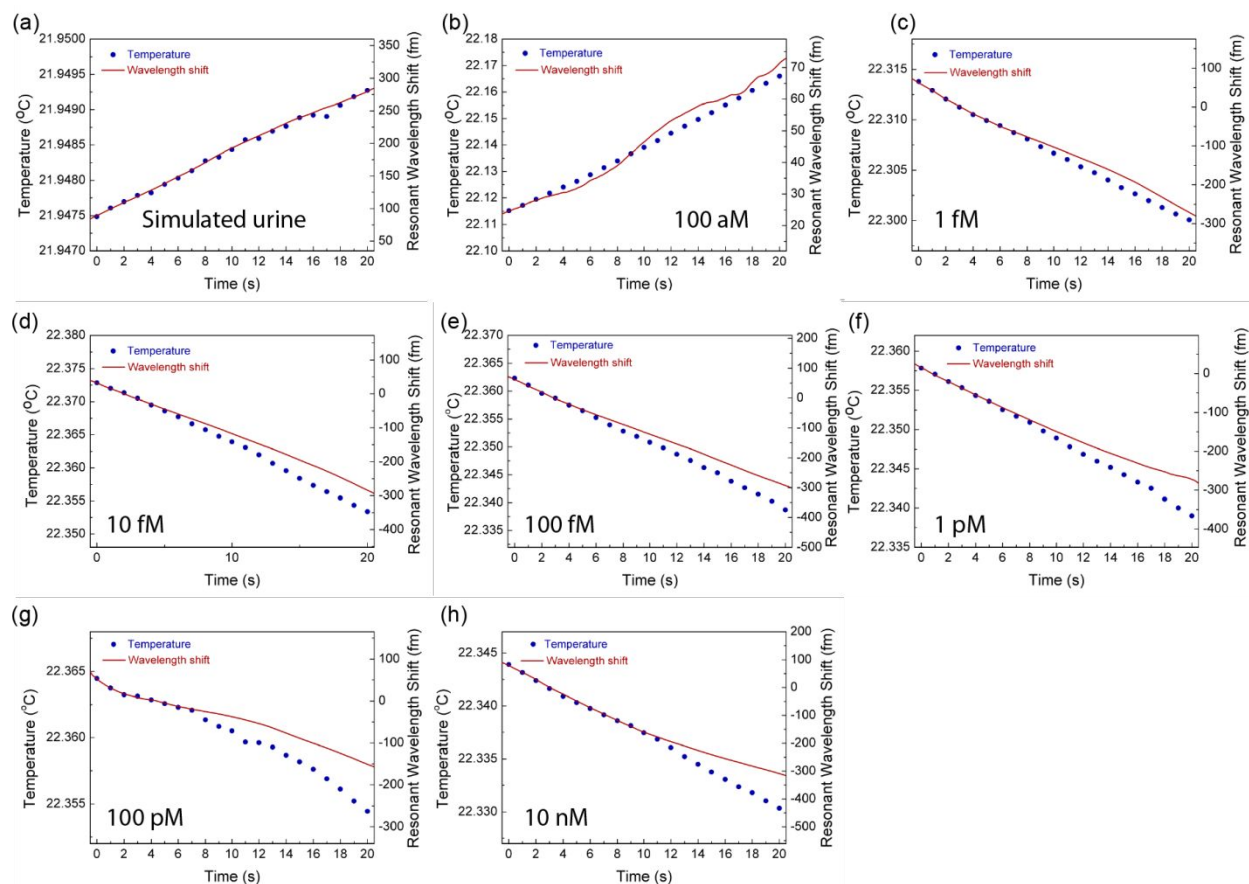


**Figure S4. Simultaneous wavelength and temperature measurement.** (a)-(h) Changes in temperature of the sample cell and resonant wavelength shifts of the toroid in response to increasing concentrations of hCG in simulated urine are measured. In panel (a), only simulated urine with no hCG present is used. The red line represents the wavelength shift of the toroid. The blue dots represent the temperature as measured by a thermocouple. Even at concentrations (e.g., 100 aM) that are slightly below our limit of detection, hCG binding generates wavelength shifts that deviate from the thermal shift measured using a thermocouple.